Identification of the Ca^{2+} Blocking Site of Acid-sensing Ion Channel (ASIC) 1: Implications for Channel Gating

Martin Paukert,[1] Elena Babini,[1] Michael Pusch,[2] and Stefan Gründer[1]

[1]Department of Physiology II, Gmelinstr. 5, D-72076 Tübingen, Germany
[2]Istituto di Biofisica, Consiglio Nazionale delle Ricerche, I-16149 Genova, Italy

ABSTRACT Acid-sensing ion channels ASIC1a and ASIC1b are ligand-gated ion channels that are activated by H^+ in the physiological range of pH. The apparent affinity for H^+ of ASIC1a and 1b is modulated by extracellular Ca^{2+} through a competition between Ca^{2+} and H^+. Here we show that, in addition to modulating the apparent H^+ affinity, Ca^{2+} blocks ASIC1a in the open state ($IC_{50} \sim 3.9$ mM at pH 5.5), whereas ASIC1b is blocked with reduced affinity ($IC_{50} > 10$ mM at pH 4.7). Moreover, we report the identification of the site that mediates this open channel block by Ca^{2+}. ASICs have two transmembrane domains. The second transmembrane domain M2 has been shown to form the ion pore of the related epithelial Na^+ channel. Conserved topology and high homology in M2 suggests that M2 forms the ion pore also of ASICs. Combined substitution of an aspartate and a glutamate residue at the beginning of M2 completely abolished block by Ca^{2+} of ASIC1a, showing that these two amino acids (E425 and D432) are crucial for Ca^{2+} block. It has previously been suggested that relief of Ca^{2+} block opens ASIC3 channels. However, substitutions of E425 or D432 individually or in combination did not open channels constitutively and did not abolish gating by H^+ and modulation of H^+ affinity by Ca^{2+}. These results show that channel block by Ca^{2+} and H^+ gating are not intrinsically linked.

KEY WORDS: epithelial Na^+ channel • ion channel • channel pore • *Xenopus* oocyte • channel gating

INTRODUCTION

Acid-sensing ion channels (ASICs) belong to the DEG/ENaC superfamily of ion channels (Waldmann and Lazdunski, 1998). Members of this supergene family form Na^+-selective ion channels (P_{Na}/P_K, 8–100), which can be blocked by amiloride (IC_{50}, 0.2–20 μM) (Alvarez de la Rosa et al., 2000; Kellenberger and Schild, 2002).

Members of the DEG/ENaC family likely have a similar overall structure. Amino acids of members of the ASIC subfamily are >45% identical to each other and ~20–25% identical to the subunits of the epithelial sodium channel (ENaC). The primary structure of all family members shows some common hallmarks, including two hydrophobic domains, short NH_2- and COOH termini, and a large loop containing conserved cysteines between the hydrophobic domains. A topology with two transmembrane-spanning domains and intracellular termini has been experimentally verified for ENaC subunits (Canessa et al., 1994; Renard et al., 1994; Snyder et al., 1994). According to the current model of the pore structure, amino acids preceding the second transmembrane (M2) domain form the binding site for amiloride (Schild et al., 1997; Sheng et al., 2000), and amino acids within the M2 domain form the selectivity filter of ENaC (Kellenberger et al., 1999a,b; Snyder et al., 1999; Sheng et al., 2000, 2001). The preM2 and the M2 domain of ASICs are almost completely conserved between different ASIC subunits and show high homology to ENaC subunits, suggesting that they contribute to the amiloride binding site and the selectivity filter of ASICs. There are, though, some differences in pore properties of ENaC and ASICs. ENaC is virtually impermeable to K^+ ($P_{Na}/P_K \sim 100$) and Ca^{2+}, and is blocked only by unphysiologically high concentrations of divalent cations ($IC_{50} > 10$ mM) (Schild et al., 1997). In contrast, ASICs discriminate less between Na^+ and K^+ ($P_{Na}/P_K \leq 15$), and ASIC1a shows a low but significant Ca^{2+} permeability ($P_{Na}/P_{Ca} \sim 15$) (Bässler et al., 2001).

ASICs are activated by a rise in the extracellular concentration of H^+. Proposed functions of ASICs include modulation of neuronal activity by extracellular pH (Waldmann and Lazdunski, 1998), peripheral perception of pain (Sutherland et al., 2001; Chen et al., 2002), and perception of taste (Ugawa et al., 2003). So far, six different members of this subfamily have been cloned (ASIC1a, ASIC1b, ASIC2a, ASIC2b, ASIC3, and ASIC4), which are encoded by four genes (Price et al.,

Address correspondence to Stefan Gründer, Department of Physiology II, Gmelinstr. 5, D-72076 Tübingen, Germany. Fax: 49-7071-29-5074; email: stefan.gruender@uni-tuebingen.de

E. Babini's present address is Istituto di Biofisica, CNR, Via de Marini 6, I-16149 Genova, Italy.

Abbreviations used in this paper: ASIC, acid-sensing ion channel; ENaC, epithelial sodium channel.

1996; Waldmann et al., 1996, 1997a,b; Garcia-Anoveros et al., 1997; Akopian et al., 2000; Gründer et al., 2000).

ASIC1b is a splice variant of ASIC1a (Chen et al., 1998; Bässler et al., 2001), in which approximately the first third of the protein is exchanged, whereas the COOH-terminal two thirds are identical. ASIC1a is expressed throughout the brain and in sensory neurons of the dorsal root ganglion (Waldmann et al., 1997a), whereas ASIC1b is specifically expressed in sensory neurons (Chen et al., 1998). Both subunits form rapidly activating and completely desensitizing ion channels ($\tau_{act} \sim 10$ ms, $\tau_{inact} \sim 1$ s) (Bässler et al., 2001) that are activated by H^+ in the physiological pH range ($pH_{0.5}$, 5.9–6.4) (Babini et al., 2002). The molecular identity of the H^+ sensor of ASICs is unknown.

We have previously shown that Ca^{2+} stabilizes the closed state of ASIC1 (Babini et al., 2002) and have proposed that Ca^{2+} binds to an extracellular site modulating the apparent affinity to H^+. Recently, Immke and McCleskey (2003) extended our findings for ASIC3 and proposed an elegant model, in which Ca^{2+} blocks the open pore. Relief of the Ca^{2+} block by the competitive binding of H^+ would open the channel, thereby accounting for H^+ gating. Thus, this model predicts that disruption of the blocking site should constitutively open the channels. The aim of this study was to further address the relation between Ca^{2+} block and H^+ gating of ASICs. We report here that substitution of two negatively charged amino acids at the beginning of the second transmembrane domain of ASIC1a reliefs Ca^{2+} block. Our results show that the relief of Ca^{2+} block is not sufficient to open the pore of ASIC1a.

MATERIALS AND METHODS

cDNAs and Site-directed Mutagenesis

cDNAs for rat ASIC1a and ASIC1b have been described previously (Bässler et al., 2001). Point mutations were introduced by recombinant PCR using Pwo DNA polymerase (Roche). In brief, two fragments were amplified with primers containing the desired mutations in an overlapping region, joined by recombinant PCR, digested by appropriate restriction endonucleases (ASIC1a: MscI/XhoI; ASIC1b: SexAI/XhoI), and ligated into the corresponding cDNA in the vector pRSSP. All PCR-derived fragments were entirely sequenced.

Whole-oocyte Electrophysiology

Using the mMessage mMachine kit (Ambion), capped cRNA was synthesized by SP6 RNA polymerase from ASIC1a, ASIC1b, and mutant cDNA, which had been linearized by NaeI. cRNA was injected into stage V to VI oocytes of *Xenopus laevis*, and oocytes were kept in OR-2 medium (concentrations in mM: 82.5 NaCl, 2.5 KCl, 1.0 Na_2HPO_4, 5.0 HEPES, 1.0 $MgCl_2$, 1.0 $CaCl_2$, and 0.5 g/l PVP) for 1–5 d. We injected 0.01–0.1 ng of ASIC1a wild-type cRNA and 1–10 ng of the other cRNAs; currents ranged from 0.5 to 20 μA.

The bath solution for two-electrode voltage clamp contained (in mM): 140 NaCl, 10 HEPES; concentrations of divalent cations ($BaCl_2$, $MgCl_2$, or $CaCl_2$) were as indicated in the figure legends. Since H^+ affinity of ASIC1 is modulated by extracellular Ca^{2+} (Babini et al., 2002), we kept the Ca^{2+} concentration always constant (1.8 mM) between low-pH activation and changed it only during low pH activation. Therefore, Ca^{2+} may not completely reach a steady-state equilibrium at its binding site during low pH activation. This may slightly affect the shape of the blocking curve and the IC_{50}. For measurements determining permeability to divalent cations, bath solution contained (in mM): 50 $BaCl_2$, 10 HEPES. pH was adjusted using NaOH or $Ba(OH)_2$; HEPES was replaced by MES buffer where appropriate. Holding potential was −60 mV or −70 mV.

Ca^{2+} blocking curves and H^+ dose–response curves were registered using an automated, pump-driven solution exchange system together with the oocyte testing carousel controlled by the interface OTC-20 (npi electronic GmbH). With this system, 90% of the solution surrounding an oocyte can be exchanged within ~100 ms. Currents were recorded with a TurboTec 03X amplifier (npi electronic GmbH) with the filter set to 20 Hz, digitized at 1 kHz using the AD/DA interface PCI 1200 (National Instruments), and stored on hard disk. Data acquisition and solution exchange were managed using the software CellWorks 5.1.1 (npi electronic GmbH). Steady-state inactivation curves were registered using gravity-driven solution exchange. Currents were recorded with a TurboTec 01C amplifier (npi electronic GmbH), data stored on hard disk, and analyzed using IgorPro software (WaveMetrics). Amiloride, EDTA, niflumic acid, and flufenamic acid were from Sigma-Aldrich.

Outside-out Patch-clamp Measurements

Oocytes injected with 1–10 ng of ASIC1a wild type or ASIC1aE425GD432C cRNA were used. Following shrinkage of oocytes in a hypertonic solution (300 mM K aspartate), the vitelline membrane was manually removed using forceps. The oocytes were allowed to recover from shrinkage for several minutes in the recording chamber containing the following solution (in mM): 100 KCl, 2 $MgCl_2$, 10 EGTA, 10 HEPES; pH was adjusted to 7.2 with KOH. This solution was also used for seal and outside-out patch formation. Thick-walled borosilicate glass capillaries (Science Products GmbH) were used to pull pipettes with a resistance of 6–10 MΩ. Patch pipettes were backfilled with a solution containing (in mM): 140 KCl, 2 $MgCl_2$, 5 EGTA, 10 HEPES; pH was adjusted to 7.4 with KOH. Following outside-out patch formation, the patch pipette was placed in front of a piezo-driven double-barreled application pipette enabling fast solution exchange (Bässler et al., 2001). Gravity-driven test and control solution flowing out of the application pipette contained (in mM): 140 NaCl, 10 HEPES; concentration of divalent cations and pH (adjusted with NaOH) were as described in RESULTS. Patches were clamped to −100 mV. Data were acquired using an Axopatch 200A amplifier (Axon Instruments), filtered with the built-in Bessel filter at 1 kHz, digitized at 10 kHz, and stored on hard disk. All experiments were conducted at room temperature.

Data Analysis

ASIC1a currents were characterized by a rundown in whole oocyte experiments (current amplitude of the eighth low-pH application ~60% of the first application); this current rundown can be appreciated in Fig. 6 B, right panel. To compensate this rundown, we always analyzed an equal number of experiments in which we measured the current amplitude with increasing and with decreasing Ca^{2+} concentrations. In addition, current values were normalized to currents that were obtained under identical experimental conditions but with identical Ca^{2+} concentration (1.3 mM) during channel activation. Current values were then

normalized to the current measured with 0.1 mM Ca^{2+} and data were fitted for each experiment using the following equation:

$$I = a + (I_{max} - a)/(1 + (IC_{50}/[B])^n), \quad (1)$$

where I_{max} is the maximal current, a is the residual current, which is insensitive to Ca^{2+} block, [B] is the concentration of Ca^{2+}, IC_{50} is the concentration at which half-maximal block occurs, and n is the Hill coefficient. This type of analysis allowed a good qualitative comparison of wild-type and mutant channels. For their quantitative comparison, we focused our analysis on the residual current with 10 mM Ca^{2+}, expressed as a fraction of the current measured with 0.1 mM Ca^{2+}. Our determination of the apparent binding constant (IC_{50}) of Ca^{2+} neglects possible contributions of surface charge and competition with Na^+ and H^+ ions to the interaction of Ca^{2+} ions with the channel protein. While such interactions likely affect the precise value of the apparent binding constant, they do not alter the fundamental conclusions of this paper that are based on the large difference of the IC_{50} of wild type and mutants.

For determination of competition between Ca^{2+} and amiloride, channels were activated every 30 s with a solution of pH 5.5 that contained increasing concentrations of amiloride. Experiments were done with the acidic solutions containing either 0.1 or 10 mM Ca^{2+} as the only divalent cation. The current amplitudes with amiloride were normalized to and then subtracted from the amplitude without amiloride to obtain the fraction of the blocked current. These data were not compensated for rundown and were fit to a Hill equation like Eq. 1.

Voltage dependence of the block was analyzed using a Boltzmann equation (Woodhull, 1973):

$$K_i(V) = K_i(0)\exp(z'FV/RT), \quad (2)$$

where $K_i(V)$ is the voltage-dependent inhibitory constant, $K_i(0)$ is the inhibitory constant at 0 mV, and z' is the product of the valence z of the blocking ion and the fraction of the membrane potential δ acting on the ion. F, R, and T have their usual meanings.

Xenopus oocytes possess an endogenous Ca^{2+}-activated Cl^- channel in their membrane. To exclude a contamination of the measured current by a Cl^- current, which could have been activated by Ca^{2+} flowing through ASIC1a, we compared the amplitude of H^+-activated currents in the presence of either Mg^{2+} or Ca^{2+} in the extracellular solution. We used concentrations of Mg^{2+} and Ca^{2+} that produced comparable block of ASIC1a (5 mM and 1.8 mM, respectively). These currents were of comparable amplitude (not depicted), demonstrating that the Ca^{2+} permeability of ASIC1a is too low to efficiently activate the Ca^{2+}-activated Cl^- channel of *Xenopus* oocytes. However, we did not systematically investigate activation of the Cl^- channel by ASIC1a. Therefore, we cannot exclude a small contribution of a Cl^- current to the total current at high extracellular Ca^{2+} concentrations or at potentials more negative than −70 mV.

Reversal potentials with extracellular Na^+ were determined by running a fast (200 ms) voltage ramp from −70 to +40 mV. Currents were leak subtracted by running the ramp before and during low pH (5.0) activation. Only oocytes with current amplitudes <2 μA were analyzed to avoid clamp artifacts. In whole cell measurements with $BaCl_2$ in the bath, we determined the current amplitude in 5-mV steps between −55 mV and −75 mV. Reversal potential was then calculated using a linear fit between the current values between which current reversed its sign.

Single-channel recordings were analyzed with the software *Ana* (available at http://www.ge.cnr.it/ICB/conti_moran_pusch/programs-pusch/software-mik.htm). Segments of channel openings from individual recordings under the same condition were pooled and contributed to the respective amplitude histogram. The amplitude distribution was fitted to a sum of Gaussian functions.

Results are reported as means ± SEM or, for the amplitude histograms, as means ± σ. They represent the mean of n individual measurements on different oocytes or different patches. For each condition, oocytes from at least two different frogs and patches from at least two different oocytes were analyzed. Statistical analysis was done with the unpaired t test.

RESULTS

Block of ASIC1 by Divalent Cations

We investigated the block by Ca^{2+} of ASIC1a and 1b expressed in *Xenopus* oocytes. Since Ca^{2+} shifts the steady-state inactivation as well as the pH activation curve (Babini et al., 2002), we held the concentration of Ca^{2+} constant (1.8 mM) between activation steps and used a saturating pH for activation that leads to full activation at all Ca^{2+} concentrations used (ASIC1a: pH 5.5; ASIC1b: pH 4.7). This acidic application solution contained varying Ca^{2+} concentrations. As is shown in Fig. 1 (A and C), increasing Ca^{2+} concentrations during channel activation reduced the current amplitude of ASIC1a progressively. 10 mM Ca^{2+} blocked 60 ± 3% of the ASIC1a current (n = 16; Fig. 1, A and C). This reduction of the current amplitude cannot be explained by incomplete recovery. With low concentrations of divalent cations (0.3 mM), recovery of ASIC1a is complete in ~1 min (Babini et al., 2002). Recovery with 1.8 mM Ca^{2+} as used in our experiments will be significantly faster (Babini et al., 2002). Since we used 1 min between activation steps, all channels should have recovered from inactivation during this time. In addition, as mentioned above, at pH 5.5, the reduction by Ca^{2+} of the current amplitude cannot be due to a shift in the dose–effect curve. Hence, most likely, Ca^{2+} blocked ASIC1a in the open conformation and is, therefore, a permeant blocker of ASIC1a. Fit to a single-site Hill equation (Eq. 1) of the Ca^{2+} dose–response curve of ASIC1a revealed a half-maximal block (IC_{50}) at 3.9 ± 1.0 mM with a Hill coefficient of 1.3 (n = 16; Fig. 1, A and C), consistent with the idea that one Ca^{2+} ion blocks ASIC1a channels. ASIC1a currents were also blocked by Ba^{2+} and Mg^{2+} (affinity for block by Ba^{2+} was similar to block by Ca^{2+}, and the affinity for block by Mg^{2+} was approximately threefold lower; not depicted) but only slightly by the divalent cations Zn^{2+} and Cd^{2+} (40 ± 2% of the current blocked by 10 mM Zn^{2+}, n = 3, and 14 ± 2% of the current blocked by 3 mM Cd^{2+}, n = 4). In contrast to ASIC1a, current amplitude of ASIC1b was only slightly reduced by Ca^{2+} (37 ± 5% of the current blocked by 10 mM Ca^{2+}, n = 8; Fig. 1, B and C).

In addition to the reduction of the current amplitude, Ca^{2+} also influenced the desensitization of

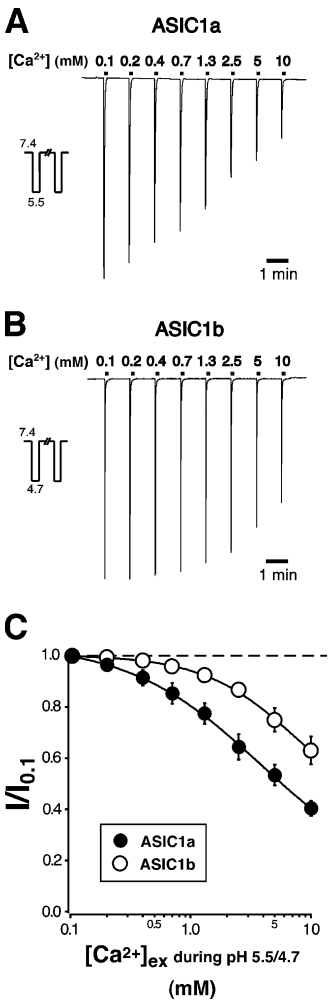

FIGURE 1. Block by Ca^{2+} of ASIC1 expressed in *Xenopus* oocytes. (A) Block by Ca^{2+} of ASIC1a. Representative trace of ASIC1a currents elicited by application of pH 5.5 and varying concentrations of extracellular Ca^{2+}. The trace was obtained from two original traces, one measured with increasing and one with decreasing Ca^{2+} concentrations. Both traces were normalized and then averaged to yield the trace shown. Acidic application solution was applied for 10 s and contained 140 mM NaCl and the indicated concentration of $CaCl_2$. Neutral bath solution was applied for 1 min between channel activation and always contained 140 mM NaCl and 1.8 mM $CaCl_2$. (B) Block by Ca^{2+} of ASIC1b. Representative trace of ASIC1b currents elicited by application of pH 4.7 and varying concentrations of extracellular Ca^{2+}. The trace was obtained by averaging two traces as described in A. Duration of solution application and concentration of NaCl and $CaCl_2$ as in A. (C) Dose–response relationship for inhibition by Ca^{2+}. Lines represent a fit of the data to Eq. 1; the dotted line represents the maximal current, $I = 1$. IC_{50} was 3.92 ± 1.02 mM ($n = 16$) for ASIC1a and >10 mM ($n = 8$) for ASIC1b. Hill coefficient was 1.25 ± 0.16 and 3.48 ± 2.58, respectively. Note that block of ASIC1a is not complete with 10 mM Ca^{2+}. Peak current amplitudes with 0.1 mM Ca^{2+} were 12.1 ± 1.6 μA for ASIC1a and 17.6 ± 4.4 μA for ASIC1b.

ASIC1a. The time constant τ of desensitization significantly decreased from τ = 2.2 ± 0.4 s with 0.1 mM Ca^{2+} to τ = 1.3 ± 0.1 s with 10 mM Ca^{2+} ($n = 9$, $P < 0.05$). Desensitization of ASIC1b was faster than desensitization of ASIC1a with 0.1 mM Ca^{2+} (τ = 0.7 ± 0.1 s), but not significantly accelerated by 10 mM Ca^{2+} (τ = 0.9 ± 0.2 s; $n = 8$, $P = 0.1$).

Ca^{2+} Reduces the Apparent Single Channel Amplitude of ASIC1a

We further confirmed that the observed inhibitory effect of Ca^{2+} on ASIC1a is due to an open channel block using single channel analysis. A low-affinity block of an ion channel pore is often associated with a flickering between the blocked and unblocked state that is faster than can be resolved by the patch-clamp technique. Therefore such a flickering block becomes apparent as a reduced single channel amplitude. A flickering block by Ca^{2+} has already been shown for ASIC3 (Immke and McCleskey, 2003). To open single channels in an outside-out patch from *Xenopus* oocytes, we switched from a control solution of pH 7.4 containing 1.8 mM Ca^{2+} and 1.0 mM Mg^{2+} to a test solution of pH 7.05 containing 1.8 mM Ca^{2+} or to a solution of pH 7.15 containing 0.1 mM Ca^{2+}. These test pH values are in the range where the steady-state inactivation curve and the pH activation curve of ASIC1a overlap (Babini et al., 2002; Fig. 6). Hence a small steady-state current can be expected at these pH values. Indeed, under these conditions, single channel openings could often be detected also several seconds after the initial channel desensitization. Fig. 2 A shows, on the left, an example trace and, on the right, the amplitude histogram that was generated from several recordings obtained from outside-out patches of ASIC1a-expressing oocytes in the presence of 1.8 mM extracellular Ca^{2+}. The histogram revealed a single channel amplitude of −1.3 ± 0.4 pA for ASIC1a wild type ($n = 4$ individual patches). Occasionally, very short current events (shorter than 2 ms) with an amplitude around 4 pA were observed that, due to their short duration, did not appear in the histogram. Frequency and duration of channel openings were variable between recordings from individual patches, not allowing the analysis of the mean open time. In contrast to the measurements with 1.8 mM Ca^{2+}, in the presence of 0.1 mM extracellular Ca^{2+}, single ASIC1a channels had an amplitude of −4.9 ± 0.9 pA (Fig. 2 B; $n = 3$ individual patches). The reduced amplitude of single ASIC1a channels with 1.8 mM Ca^{2+} compared with 0.1 mM Ca^{2+} confirms that Ca^{2+} is an open channel blocker of ASIC1a.

A reduction of the single channel amplitude from −4.9 pA with 0.1 mM Ca^{2+} to −1.3 pA with 1.8 mM Ca^{2+} predicts an apparent Ca^{2+} affinity of the blocking site that is considerably higher than 3.9 mM, the value obtained by the voltage clamp analysis on whole oocytes. We explain this apparent discrepancy by a pH-

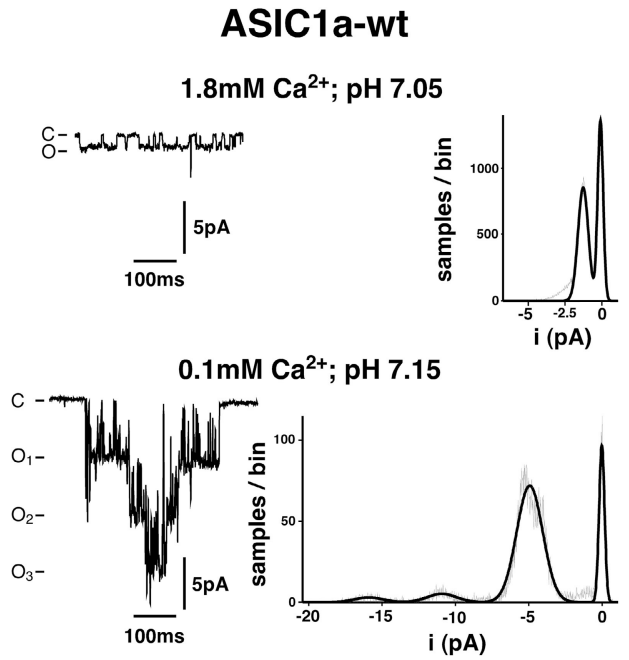

FIGURE 2. Apparent single channel amplitude of ASIC1a depends on extracellular Ca^{2+}. (Top) Single channel current amplitude of ASIC1a with 1.8 mM Ca^{2+}. Left, representative segment of an outside-out patch-clamp recording. The extracellular test solution contained 140 mM NaCl and 1.8 mM $CaCl_2$; pH was 7.05. Right, amplitude histogram representing the respective pool of segments of recordings as shown on the left; 299 individual events contributed to the histogram. Amplitude distribution was fitted to a sum of Gaussian functions. Single channel current amplitude was -1.3 ± 0.4 pA (mean $\pm$ σ; $n = 4$ individual patches). Holding potential was -100 mV. (Bottom) Single channel current amplitude of ASIC1a with 0.1 mM Ca^{2+}. Left, representative segment of an outside-out patch-clamp recording. Right, amplitude histogram; 165 individual events of level 1 (corresponding to one open channel) contributed to the histogram. Single channel current amplitude was -4.9 ± 0.9 pA ($n = 3$ individual patches). Holding potential was -100 mV.

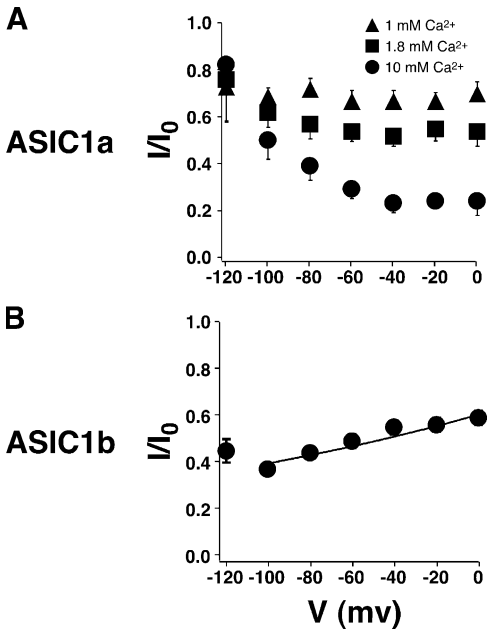

FIGURE 3. Voltage dependence of Ca^{2+} block in ASIC1. (A) Voltage dependence of Ca^{2+} block of ASIC1a. Current measured with 1 mM, 1.8 mM, or 10 mM Ca^{2+} was normalized to the current measured with 0 mM Ca^{2+} (I_{xCa}/I_{0Ca}) at a given holding potential ($n = 8$). (B) Voltage dependence of Ca^{2+} block in ASIC1b. Current measured with 10 mM Ca^{2+} was normalized to the current measured with 0 Ca^{2+}. Fit of the data from 0 mV to 100 mV to a Boltzmann function is represented by the line and gave a δ value of 0.054 ± 0.007 ($n = 9$).

dependence of the Ca^{2+} affinity of the blocking site. As shown below, we identified aspartate and glutamate residues as crucial components of the Ca^{2+} blocking site. We propose that neutralization of the side chains of these amino acids by the low pH used for activation of ASIC1a will reduce the apparent affinity to Ca^{2+}. Since we used lower pH for the whole cell experiments than for the patch clamp experiments, the affinity to Ca^{2+} will appear lower in the whole cell experiments than in the patch clamp experiments (see DISCUSSION).

Voltage Dependence of Ca^{2+} Block

Next, we determined the voltage dependence of Ca^{2+} block. Block of ASIC1a was decreased at hyperpolarized potentials with Ca^{2+} concentrations ranging from 1 to 10 mM (Fig. 3 A). Since ASIC1a is not only blocked by Ca^{2+} but also permeable for Ca^{2+} (Bässler et al., 2001), this most likely reflects a voltage dependence of the Ca^{2+} permeation. For the Ca^{2+}-impermeable ASIC1b, the voltage dependence of Ca^{2+} block was investigated only for a Ca^{2+} concentration of 10 mM, which significantly blocked ASIC1b (Fig. 1, B and C). In contrast to ASIC1a, block of ASIC1b was slightly increased at hyperpolarized potentials (Fig. 3 B). Only at potentials more negative than -100 mV was a decreased block observed, which is most likely due to some unspecific Ca^{2+} influx at this strong hyperpolarization with the high Ca^{2+} concentration. By fitting the voltage dependence between 0 mV and -100 mV to a Boltzmann function (Eq. 2), we estimated the fraction of the transmembrane electric field sensed by the blocking Ca^{2+} ion to be $\sim$5% ($\delta = 0.054 \pm 0.007$, $n = 9$). Together, our results show that Ca^{2+} block of ASIC1 does not strongly depend on voltage, suggesting a binding site outside the deep parts of the membrane-spanning regions of the channel and therefore most likely outside the narrow part of the ion pore.

Identification of the Ca^{2+} Binding Site

Since the second transmembrane domain M2 is supposed to line the ion pore, we considered amino acids preceding M2 or at the beginning of M2 as candidate

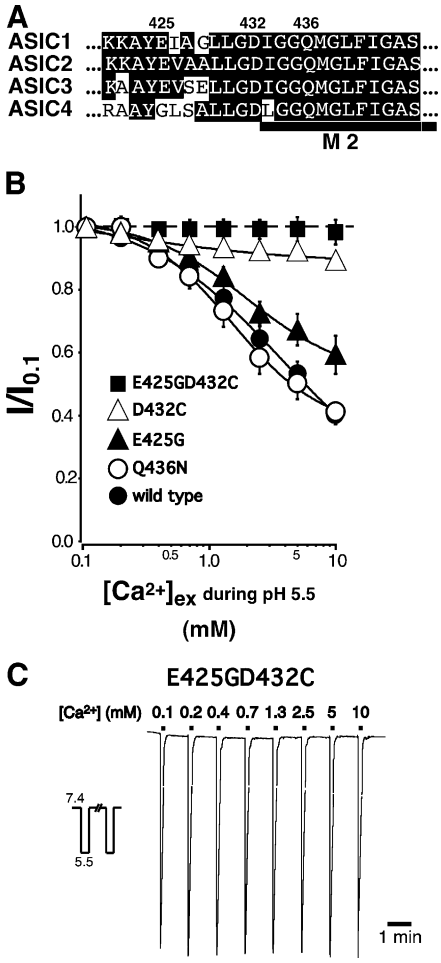

FIGURE 4. Combined mutation of glutamate 425 and aspartate 432 of ASIC1a abolishes Ca^{2+} block. (A) Amino acid sequences of the predicted second transmembrane domain M2 of ASICs in the one-letter code. Amino acids in M2 are identical between ASIC1a and ASIC1b. The position of M2 is indicated by the bar. (B) Dose–response curves for Ca^{2+} block of ASIC1a channels containing the E425G, the D432C, the Q436N, or the E425GD432C substitution. Recordings were obtained using the same protocol as described for Fig. 1. Current that was blocked by 10 mM Ca^{2+} was 59 ± 3% (n = 12) for Q436N, 41 ± 6% (n = 12) for E425G, 11 ± 2% (n = 14) for D432C, and 2 ± 4% (n = 14–16) for E425GD432C. Lines represent a fit to a logistic function (Eq. 1) of the mean data for individual Ca^{2+} concentrations. Dose–response curve for Ca^{2+} block of ASIC1a wild type from Fig. 1 is shown for comparison. Peak current amplitudes with 0.1 mM Ca^{2+} were 17.9 ± 3.1 μA for Q436N, 6.5 ± 1.0 μA for E425G, 5.8 ± 0.5 μA for D432C, and 7.7 ± 1.0 μA for E425GD432C. (C) Representative trace of ASIC1aE425GD432C currents elicited by application of pH 5.5 and varying concentrations of extracellular Ca^{2+}. The trace was obtained by averaging two original traces as described for Fig. 1 A. Duration of solution application and concentration of NaCl and $CaCl_2$ as in Fig. 1 A.

blocking sites. M2 of ASIC1a was predicted to begin at isoleucine 433 (I433) (TMpred at http://www.ch.embnet.org/). This prediction is in good agreement with experimental data for other ion channels of the DEG/ENaC gene family (see DISCUSSION). We therefore considered glutamate 425 (E425), aspartate 432 (D432), and glutamine 436 (Q436) as possible binding sites for Ca^{2+} (Fig. 4 A). We replaced E425 by a glycine (E425G), an amino acid that is found in several other members of the supergene family, D432 by a cysteine (D432C), and Q436 by an asparagine (Q436N), a conservative substitution. For mutant Q436N, 59 ± 3% of the current was blocked by 10 mM Ca^{2+}, similar to ASIC1a wild type (IC_{50} = 2.4 ± 1.0 mM, n = 12; Fig. 4 B). Mutant channels containing either substitution E425G or D432C, however, showed a significant reduction of Ca^{2+} block ($P < 0.005$ for 10 mM Ca^{2+}). Only ~41 ± 6% of the currents through channels containing the E425G substitution were blocked by 10 mM Ca^{2+}, and only ~11 ± 2% of the currents through channels containing the substitution D432C (Fig. 4 B). The apparent affinity of Ca^{2+} block was slightly lower for mutant E425G than for the wild type (IC_{50} = 5.1 ± 2.4 mM, n = 12). For mutant D432C, the apparent Ca^{2+} affinity could not be determined with fidelity since the block by Ca^{2+} of this mutant was too weak. Since no individual mutation completely relieved Ca^{2+} block of ASIC1a, we also engineered a channel that contained both substitutions together. Channels containing the double substitution of E425 and D432 (ASIC1aE425GD432C) were not at all blocked by Ca^{2+} up to 10 mM (n = 14–16, Fig. 4 B), suggesting that both amino acids contribute to the blocking site for Ca^{2+}.

Since substitution of D432 had the strongest effect on Ca^{2+} block, we additionally replaced D432 by an alanine (mutant D432A), an asparagine (D432N), a glutamate (D432E), a valine (D432V), a leucine (D432L), and a lysine (D432K). Mutant D432A was only weakly blocked by Ca^{2+} (7 ± 3% of the current blocked by 10 mM Ca^{2+}, n = 14), similar to D432C. Mutants D432N and D432E showed rather low current amplitude and were, therefore, not analyzed in detail. Substitutions D432V, D432L, and D432K could not be activated by low pH. They also did not increase the background current, suggesting that these channels were not constitutively active (see below). The reason for the nonfunctionality of these mutant channels is not known. Also, since the functional mutants showed significantly reduced current amplitude compared with the wild type (~100-fold higher cRNA concentrations induced a similar current amplitude), it may be due to impaired surface expression. Alternatively, nonfunctionality of these mutants may be due to a strong constriction of the ion permeation pathway or to some effect on channel gating. Finally, substitution of the corresponding aspartate in ASIC1b (D465N) also further reduced Ca^{2+} block in ASIC1b (unpublished data). Due to the low expression of channels mutated at position 432, we were unable to determine the Ca^{2+} depen-

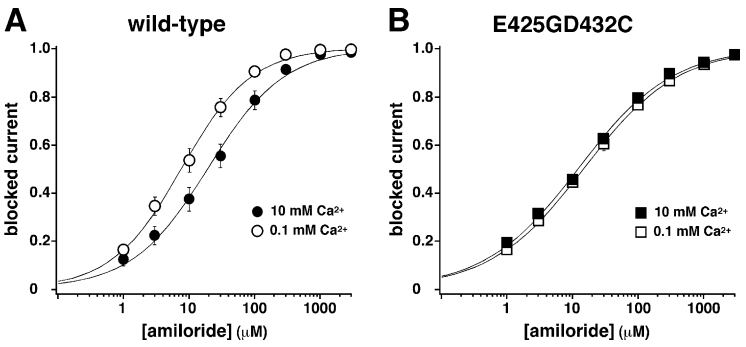

FIGURE 5. Apparent affinity for amiloride of ASIC1a wild type but not of ASIC1a E425GD432C depends on Ca^{2+}. (A) Dose–response relationship for inhibition of ASIC1a by amiloride in the presence of 0.1 mM Ca^{2+} (○) or 10 mM Ca^{2+} (●). Lines represent a fit of the data to Eq. 1. IC_{50} was 11.6 ± 2.4 μM (n = 15) in the presence of 0.1 mM Ca^{2+} and 33.3 ± 10.0 μM (n = 15) in the presence of 10 mM Ca^{2+}; $P < 0.05$. Peak current amplitudes without amiloride were 14.8 ± 1.3 μA with 0.1 mM Ca^{2+} and 10.5 ± 1.7 μA with 10 mM Ca^{2+}. Holding potential was −70 mV. (B) Dose–response relationship for inhibition of ASIC1a E425GD432C by amiloride in the presence of 0.1 mM Ca^{2+} (□) or 10 mM Ca^{2+} (■). IC_{50} was 17.2 ± 3.7 μM (n = 14) in the presence of 0.1 mM Ca^{2+} and 18.4 ± 3.9 μM (n = 14) in the presence of 10 mM Ca^{2+}; $P = 0.99$. Peak current amplitudes without amiloride were 8.1 ± 1.1 μA with 0.1 mM Ca^{2+} and 9.2 ± 1.5 μA with 10 mM Ca^{2+}. Holding potential was −70 mV.

dence of the apparent single channel amplitude for the double mutant ASIC1a E425GD432C.

Competition Between Ca^{2+} and Amiloride in ASIC1a Wild Type but Not In ASIC1a E425GD432C

We next assessed if there is a competition between the open channel blocker amiloride and Ca^{2+} and if this competition is influenced by the E425GD432C mutation. In ASIC1a wild-type channels, Ca^{2+} reduced the apparent affinity for amiloride. In the presence of 0.1 mM Ca^{2+}, amiloride blocked ASIC1a with an IC_{50} of 11.6 ± 2.4 μM (n = 15), while in the presence of 10 mM Ca^{2+}, the IC_{50} was slightly but significantly increased to 33.3 ± 10.0 μM (n = 15, $P < 0.05$; Fig. 5 A). This result is consistent with the idea of a competition between Ca^{2+} and amiloride at the entrance to the ion pore. In contrast, in the E425GD432C substitution, amiloride block was hardly affected by Ca^{2+} (IC_{50} = 17.2 ± 3.7 μM with 0.1 mM Ca^{2+} and IC_{50} = 18.4 ± 3.9 μM with 10 mM Ca^{2+}, n = 14, $P = 0.99$). Thus, in the ASIC1a E425GD432C mutant channel, a competition between Ca^{2+} and amiloride was no longer observed, lending additional support to the interpretation that E425 and D432 contribute to a binding site for Ca^{2+} at the outer entrance to the ion pore.

Substitution of D432 and E425 Does Not Prevent Modulation of H^+ Affinity by Ca^{2+}

The basic gating characteristics of ASICs were preserved in the ASIC1a substitutions E425G, D432C, and the double-substitution E425GD432C. First, channels containing these substitutions were not constitutively active (see also below) and were activated by extracellular acidification. As can be seen from Figs. 4 and 6, a rise in the extracellular H^+ concentration induced a transient inward current, similar to ASIC1a wild type. Second, steady-state inactivation and pH activation curves were still modulated by Ca^{2+}. As can be seen from Table I and Fig. 6, for all three mutants, the apparent H^+ affinity was decreased by increasing Ca^{2+}

TABLE I

Ca^{2+} Dependence of Apparent H^+ Affinity (pH_{50}) of ASIC1a Wild-type and Mutant Channels

	Wild-type	E425G	D432C	E425GD432C
pH_{50} activation				
1.8 mM Ca^{2+}/1.0 mM Mg^{2+}	6.46 ± 0.04	6.29 ± 0.05	6.23 ± 0.09	6.09 ± 0.07
n	16	23	24	26
0.1 mM Ca^{2+}	6.80 ± 0.04[c]	6.63 ± 0.05[c]	6.43 ± 0.08	6.32 ± 0.08[a]
n	16	24	24	23
pH_{50} steady-state inactivation				
1.8 mM Ca^{2+}	7.24 ± 0.01	7.18 ± 0.04	7.23 ± 0.01	6.95 ± 0.02
n	12	7	6	9
0.1 mM Ca^{2+}	7.48 ± 0.02[c]	7.35 ± 0.02[b]	7.48 ± 0.04[c]	7.23 ± 0.07[c]
n	12	6	4	6

Data are mean ± SEM for the indicated number of individual oocytes. Values obtained with 0.1 mM Ca^{2+} (during low pH activation for the pH_{50} activation or during the conditioning pH for the pH_{50} steady-state inactivation) were compared with values obtained with physiologic concentrations of Ca^{2+}. Values for steady-state inactivation of ASIC1a wild type were published previously (Babini et al., 2002).

[a]$P < 0.05$.

[b]$P < 0.01$.

[c]$P < 0.001$, unpaired t test.

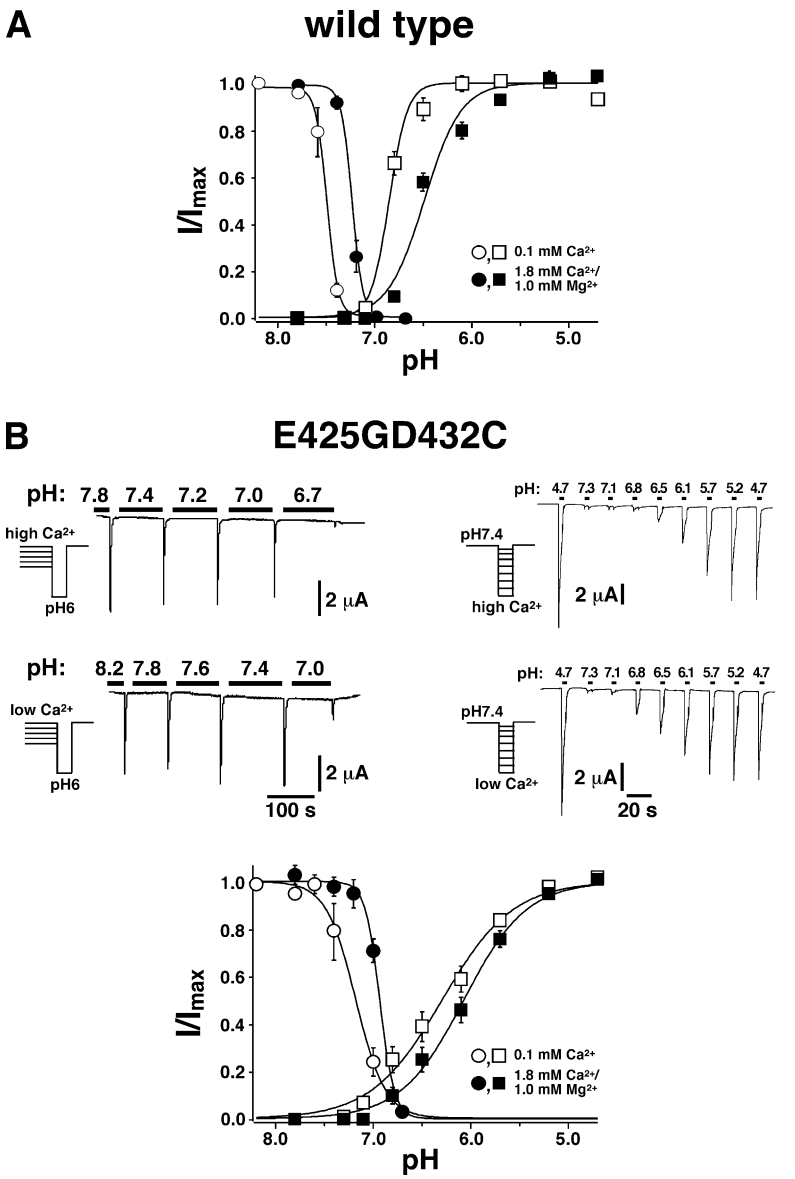

FIGURE 6. Channels containing the double substitution E425GD432C still show Ca^{2+}-dependent shifts of steady-state inactivation and pH activation curves. (A) Dose–response curves for steady-state inactivation by H^+ and for activation by H^+ with different Ca^{2+} concentrations for ASIC1a wild type. The curve for steady-state inactivation was published previously (Babini et al., 2002). For steady-state inactivation curves, oocytes were preincubated for 2 min at a conditioning pH varying between 8.2 and 6.7. After this preincubation, available channels were activated by switching to a solution of pH 6.0 containing 140 mM NaCl, 1.8 mM $CaCl_2$/1.0 mM $MgCl_2$. The preincubation solution contained 140 mM NaCl and either 1.8 mM $CaCl_2$/1.0 mM $MgCl_2$ (●) or 0.1 mM $CaCl_2$ (○). The preincubation solution with 0.1 mM $CaCl_2$ also contained 0.1 mM niflumic acid to block the large conductance induced in oocytes by divalent-free extracellular solutions. For H^+ activation curves, the preincubation solution contained 140 mM NaCl, 1.8 mM $CaCl_2$/1.0 mM $MgCl_2$; pH 7.8. Every 30 s, a test solution with a pH ranging from 7.4 to 4.7 was applied for 3 s. The test solution contained 140 mM NaCl and either 1.8 mM $CaCl_2$/1.0 mM $MgCl_2$ (■) or 0.1 mM $CaCl_2$ (□). (B) Top left, representative traces of ASIC1aE425GD432C currents showing steady-state inactivation at two different Ca^{2+} concentrations. Top right, representative traces of ASIC1aE425GD432C currents showing activation by H^+ at two different Ca^{2+} concentrations. pH was as indicated. Duration of solution application and concentration of NaCl and $CaCl_2$ were as described in A. Bottom, dose–response curves for steady-state inactivation and activation with different Ca^{2+} concentrations for ASIC1aE425GD432C.

concentrations. This decrease was in all cases significant ($P < 0.05$), except for the activation curves of D432C ($P = 0.09$). However, also for this substitution, the shift by Ca^{2+} of the H^+ sensitivity of steady-state inactivation was highly significant ($P < 0.001$).

However, there were also notable changes in the gating properties of these substitutions. First, the apparent H^+ affinity of the substituted variants was more acidic than of the wild-type channel (Table I, $P < 0.05$ for pH activation). Second, the Hill coefficient of the activation curves was smaller (1.9 ± 0.1 for E425GD432C compared with 2.9 ± 0.3 for the wild type with physiologic concentrations of divalent cations, $P < 0.005$), possibly indicating the loss of one or more H^+ binding sites. And finally, the Ca^{2+}-induced shift of the curves was smaller than for the wild-type channel (Table I), possibly indicating the loss of a Ca^{2+} binding site.

Other Pore Properties of Substitutions at D432 or E425

We also addressed the question whether substitutions at D432 or E425 influenced other pore properties. First, we investigated ion selectivity by running a voltage ramp from −70 mV to +40 mV. The extracellular solution contained 40 mM NaCl and 100 mM NMDGCl in order to shift the Na^+ equilibrium potential to less positive values and to avoid activation of the large depolarization-induced Na^+ conductance that is endogenous to oocytes (Baud et al., 1982). Reversal potentials were significantly less positive for both D432C and E425G than for the wild type (E_{rev}, 22.1 ± 4.5 mV for ASIC1a wild type, 7.0 ± 6.7 for D432C, and 15.1 ± 7.6 for E425G, $n = 10$–17; $P < 0.05$), indicating a 1.5–2-fold reduction of the relative permeability P_{Na}/P_K. Next, we addressed if the apparent loss of the Ca^{2+} block by sub-

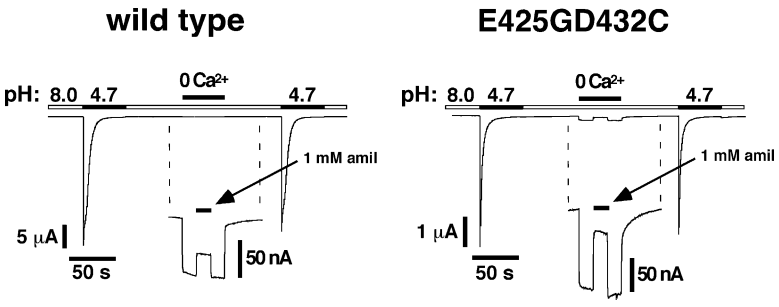

FIGURE 7. Removal of extracellular Ca^{2+} opens ASIC1aE425GD432C. ASIC1a channels were first activated by pH 4.7. 60 s after recovery in pH 8.0, a solution containing no Ca^{2+} and no Mg^{2+}, but 10 mM EDTA was applied; the concentration of Ca^{2+} in this solution should be in the low picomolar range. As can be seen from the blow-up, this divalent-free solution induced a small amiloride-sensitive current in ASIC1a wild type–expressing oocytes (left) as well as in E425GD432C-expressing oocytes (right). A similar response was seen in six independent oocytes for each condition. Solutions contained 0.2 mM flufenamic acid to block the large conductance induced in oocytes by divalent-free extracellular solutions.

stitutions of D432 and E425 could be due to an increased permeability to Ca^{2+}. Since any strong increase in the Ca^{2+} permeability should be accompanied by an increase in the Ba^{2+} permeability, we assessed the Ca^{2+} permeability of the mutants indirectly using 50 mM Ba^{2+} as the only cation in the bath solution. Under these conditions, ASIC1a currents reversed at a potential of −66.3 mV ± 4.6 mV (n = 6), as has previously been reported (Bässler et al., 2001). Since mutants ASIC1aD432C and ASIC1aE425G were characterized by reduced current amplitude, only a few measurements could be analyzed using Ba^{2+} as the main charge carrier. In these measurements, the reversal potential was slightly more negative than for the wild type (−70.9 mV ± 0.3 mV, n = 2, and −78.8 mV ± 4.3 mV, n = 4, respectively), indicating that the permeability to divalent cations was not increased by these substitutions.

Channels Containing the E425 and the D432 Substitutions Can Be Opened by Removal of Extracellular Ca^{2+}

Recently, it has been shown that complete removal of extracellular Ca^{2+} opens ASIC3 channels (Immke and McCleskey, 2003). To address whether complete removal of extracellular Ca^{2+} also opens ASIC1a channels, we superfused oocytes with a solution that was nominally free of Ca^{2+} and in which any residual Ca^{2+} was chelated by the addition of EDTA. Superfusion of the oocytes with this solution indeed opened ASIC1a channels as can be seen in Fig. 7 from the appearance of a small current that was sensitive to block by amiloride (1 mM). The small current amplitude after removal of Ca^{2+} compared with the amplitude after activation with H^+ has also been observed for ASIC3 (Immke and McCleskey, 2003) and has been attributed to the existence of two open states, a protonated one that makes large current and a deprotonated one that makes small current (Immke and McCleskey, 2003). The current induced by removal of Ca^{2+} did not desensitize at pH 8.0 but at pH 7.4 (unpublished data). This behavior is similar to the behavior described for ASIC3 after removal of Ca^{2+}. In noninjected control oocytes, removal of Ca^{2+} did not induce a current (unpublished data).

ASIC1a substitutions E425G, D432C, and the double substitution E425GD432C were not constitutively active, since they did not induce any amiloride-sensitive current at neutral pH in a Ca^{2+}-containing solution (unpublished data). Since the Ca^{2+} blocking site had been disrupted by the double substitution, this finding indicates that removal of the Ca^{2+} ion that blocks the pore is not sufficient to open the channel. This reasoning predicts that another Ca^{2+} ion is bound to the channel and inhibits its activity. We could confirm this prediction by superfusion of oocytes expressing the double substitution E425GD432C with a Ca^{2+}-free solution. This Ca^{2+}-free solution also opened these mutant channels (Fig. 7). The current induced by removal of Ca^{2+} was amiloride sensitive (Fig. 7) and did not desensitize at pH 8.0 but at pH 7.4 (not depicted). Thus, we conclude that the mutant channels still had a Ca^{2+} ion bound and that binding of this Ca^{2+} ion did inhibit channel activity. Removal of this Ca^{2+} ion, which did not block the open pore, was sufficient to open ASIC1a.

DISCUSSION

Identification of the Ca^{2+} Blocking Site

In this study we identify two amino acids that are crucial for the block of ASIC1a by Ca^{2+}: E425 and D432. The evidence for this conclusion is twofold. First, combined substitution of E425 and D432 completely abolished Ca^{2+} block in whole cell experiments. Second, combined substitution of E425 and D432 abolished the reduction by Ca^{2+} of the apparent affinity for amiloride. As discussed in the next paragraph, D432 is most likely located at the entrance to the ion pore. Since this is an ideal location for a blocking site, we propose that D432 and E425 are part of a binding site for Ca^{2+}.

Several observations support the assumption that D432 is located at the entrance to the ion pore. First, amiloride binds within the pore of ENaC close to a residue that corresponds to G438 of ASIC1a (Schild et al., 1997). Since amiloride senses between 15 and 30% of the transmembrane electric field (Palmer, 1985; McNicholas and Canessa, 1997; Fyfe and Canessa, 1998),

this residue should be located within the electric field. Second, a Ca^{2+} binding site that had been engineered in ENaC at a residue corresponding to G435 of ASIC1a leads to a Ca^{2+} block in which Ca^{2+} senses 15% of the transmembrane electric field (Schild et al., 1997). Therefore, this residue should also be located within the electric field. Assuming an overall conserved topology of the ion pore between ASICs and ENaC and considering the slight voltage dependence that we measured for the block of ASIC1b, the mentioned results suggest that D432 is located just at the level of the beginning of the transmembrane electric field. We propose that D432 constitutes the beginning of M2. Thus, D432 would form a ring of negative charges around the entrance to the ion pore.

E425 would form a similar ring of negative charges just slightly more toward the extracellular milieu. Although we observed the strongest reduction of Ca^{2+} block with substitutions of D432, block was completely abolished only by the combined substitution of both D432 and E425. We propose that Ca^{2+} binding to either site blocks the channel. Binding to D432 more strongly blocks the channel perhaps because the pore diameter is smaller at this location and Ca^{2+} therefore constricts the ion pore more strongly. But the apparent difference with respect to Ca^{2+} block of substitutions at E425 or D432 may also be due to a different pK_a of the side chain of these amino acids (see below).

Several other studies have previously reported a block of ASIC1 by Ca^{2+} (Waldmann et al., 1997a; de Weille and Bassilana, 2001; Zhang and Canessa, 2002). In particular, a decrease of the single channel conductance by Ca^{2+} was reported (de Weille and Bassilana, 2001; Zhang and Canessa, 2002).

Relation of Ca^{2+} Block and Channel Gating by H^+

One inherent technical problem when studying Ca^{2+} block with a channel that is activated by H^+ is that the blocking site itself is modified by H^+. The pK_a of the side chain of free glutamate is ~4.3 and that of free aspartate is ~3.9. Thus, the pH that we used to activate ASICs in the whole cell experiments (pH 5.5) is close to the pK_a of these amino acids. Considering that the pK_a of these side chains may well be larger in a protein where several negative charges are in close proximity, it is likely that part of the negative charges of D432 and E425 had been neutralized by the low pH used to activate ASIC1a. Thus, activation of ASICs by H^+ will interfere with Ca^{2+} block. There are several observations that strongly support this notion. First, in our single channel experiments, unitary current amplitude was more strongly reduced by 1.8 mM Ca^{2+} compared with 0.1 mM Ca^{2+} than we expected from the whole cell experiments (by ~75%; expected was ~25%). There are several possible explanations for this apparently increased Ca^{2+} affinity in the single channel experiments compared with the whole cell experiments. However, we believe that it is most likely due to the higher pH used to activate channels in the single channel experiments compared with the pH used to activate channels in the whole cell experiments (pH 7.05 compared with pH 5.5). This also suggests that at pH 7.4, physiologic concentrations of Ca^{2+} may completely block ASICs (see below). Second, in the whole cell experiments, even 10 mM Ca^{2+} did not completely block the channel. The incomplete block also with a saturating Ca^{2+} concentration was not unexpected for a Ca^{2+}-permeable channel like ASIC1a. However, since Ca^{2+} permeability of ASIC1a is low (Bässler et al., 2001), we expected a stronger block. And finally, the block of ASIC1b was less complete than block of ASIC1a, although the putative pore-forming region M2 is identical between both channels. Since ASIC1b is less sensitive to H^+, we had to use a more acidic pH for its activation than for ASIC1a (pH 4.7 rather than pH 5.5). This will probably have neutralized more of the negative charges of the blocking sites. On the same line, in preliminary experiments (unpublished data), we did not observe a strong Ca^{2+} block of ASIC2a. However, the amino acids that mediate Ca^{2+} block in ASIC1a are conserved in ASIC2a. This apparent discrepancy can again be explained by the fact that we used pH 4.0 to activate ASIC2a. All these observations are consistent with the idea that increasing H^+ concentrations decrease the apparent Ca^{2+} affinity of the blocking site.

Recently, Immke and McCleskey (2003) proposed a detailed model to explain the opening of the ion pore of ASIC3. Their model predicts a complete block of ASIC3 by Ca^{2+} at neutral pH. The block would be achieved by binding of Ca^{2+} to a ring of negative charges at the outer mouth of the ion pore. Titration of the negative charges by H^+ would relieve the Ca^{2+} block, thereby opening the ASIC3 ion pore without accompanying conformational changes. This single Ca^{2+} binding site could explain both block of the channel as well as modulation of its apparent H^+ sensitivity by Ca^{2+}. Its simplicity makes this model very attractive. Several basic findings of Immke and McCleskey could be confirmed in the present study for ASIC1a. However, our results clearly show that a single Ca^{2+} binding site is not sufficient to explain the activation of ASIC1a by H^+. We present strong evidence that E425 and D432 are crucial parts of the Ca^{2+} blocking site. Yet, disruption of this site did not constitutively open ASIC1 channels as would be expected from the Immke-McCleskey model. Moreover, ASIC1 channels without a Ca^{2+} blocking site retained the principal gating characteristics of ASIC1 wild-type channels: activation by H^+ and modulation of the apparent H^+ affinity by Ca^{2+}. However, there is some evidence indicating that the blocking site does in-

deed contribute to the opening of ASIC1 wild-type channels by H^+. First, the shift of the apparent H^+ affinity to more acidic values of channels without the Ca^{2+} blocking site as well as the decreased Hill coefficient of the activation curve suggest the loss of a H^+ binding site. And second, the reduced shift by Ca^{2+} of the H^+ activation curve of these channels suggests the loss of a Ca^{2+} binding site. In other words, the loss of a H^+ and a Ca^{2+} binding site at the blocking site has direct impact on the activation curve. Thus, the blocking site likely contributes to the activation of ASICs by H^+ but it cannot fully account for it. As outlined below, we explain this with the presence of a second site that binds H^+ and Ca^{2+} in a competitive manner.

We show that channels without a Ca^{2+} blocking site can be slightly opened by complete removal of extracellular Ca^{2+}. This finding as well as the remaining Ca^{2+} modulation of the apparent H^+ affinity predicts another binding site for Ca^{2+}. We would like to call this other site the modulating site to distinguish it from the blocking site that we identified in this study. Binding of Ca^{2+} to the modulating site competes with the binding of H^+ to the channel, just as binding of Ca^{2+} to the blocking site does. Thus, the apparent affinity to Ca^{2+} of the two sites depends on the pH. We previously estimated the apparent Ca^{2+} affinity of the modulating site at pH 7.4 to be ~2 mM (Babini et al., 2002). Thus, the modulating site would be a low-affinity site. We determined in the present study the apparent Ca^{2+} affinity of the blocking site to also be in the low millimolar range at pH 5.5. But at pH 7.05/7.15, as used for the single channel experiments, it was already considerably higher. Immke and McCleskey estimated the apparent affinity to Ca^{2+} of the blocking site of ASIC3 to be in the low micromolar range at pH 7.4 (Immke and McCleskey, 2003). Thus, it seems that the blocking site is a high-affinity site.

In addition to the existence of a second Ca^{2+} binding site, the modulating site, our study also suggests the existence of a second H^+ binding site. This site would account for the H^+ gating of channels without a blocking site and is probably identical to the modulating site. We believe that binding of H^+ to the modulating site will not unblock the channel but rather that it releases Ca^{2+} from this site, which may induce a conformational change that opens the channel. The molecular identification of the modulating site will therefore further increase our understanding of the molecular mechanism of H^+ gating of ASICs and of the role of Ca^{2+} for gating.

We thank H.-S. Geisler and M. Siba for expert technical assistance.

This work was supported by grants of the Attempto research group program of the Universitätsklinikum Tübingen (FG 1-0-0) and the DFG (GR1771) to S. Gründer, and the Italian "Ministero dell'Istruzione, dell'Università e della Ricerca" (FIRB RBAU01PJMS) to M. Pusch.

Olaf S. Andersen served as editor.

Submitted: 6 November 2003
Accepted: 18 August 2004

REFERENCES

Akopian, A.N., C.C. Chen, Y. Ding, P. Cesare, and J.N. Wood. 2000. A new member of the acid-sensing ion channel family. *Neuroreport.* 11:2217–2222.

Alvarez de la Rosa, D., C.M. Canessa, G.K. Fyfe, and P. Zhang. 2000. Structure and regulation of amiloride-sensitive sodium channels. *Annu. Rev. Physiol.* 62:573–594.

Babini, E., M. Paukert, H.S. Geisler, and S. Gründer. 2002. Alternative splicing and interaction with di- and polyvalent cations control the dynamic range of acid-sensing ion channel 1 (ASIC1). *J. Biol. Chem.* 277:41597–41603.

Bässler, E.L., T.J. Ngo-Anh, H.S. Geisler, J.P. Ruppersberg, and S. Gründer. 2001. Molecular and functional characterization of acid-sensing ion channel (ASIC) 1b. *J. Biol. Chem.* 276:33782–33787.

Baud, C., R.T. Kado, and K. Marcher. 1982. Sodium channels induced by depolarization of the *Xenopus laevis* oocyte. *Proc. Natl. Acad. Sci. USA.* 79:3188–3192.

Canessa, C.M., A.M. Merillat, and B.C. Rossier. 1994. Membrane topology of the epithelial sodium channel in intact cells. *Am. J. Physiol.* 267:C1682–C1690.

Chen, C.C., S. England, A.N. Akopian, and J.N. Wood. 1998. A sensory neuron-specific, proton-gated ion channel. *Proc. Natl. Acad. Sci. USA.* 95:10240–10245.

Chen, C.C., A. Zimmer, W.H. Sun, J. Hall, and M.J. Brownstein. 2002. A role for ASIC3 in the modulation of high-intensity pain stimuli. *Proc. Natl. Acad. Sci. USA.* 99:8992–8997.

de Weille, J., and F. Bassilana. 2001. Dependence of the acid-sensitive ion channel, ASIC1a, on extracellular Ca^{2+} ions. *Brain Res.* 900:277–281.

Fyfe, G.K., and C.M. Canessa. 1998. Subunit composition determines the single channel kinetics of the epithelial sodium channel. *J. Gen. Physiol.* 112:423–432.

Garcia-Anoveros, J., B. Derfler, J. Neville-Golden, B.T. Hyman, and D.P. Corey. 1997. BNaC1 and BNaC2 constitute a new family of human neuronal sodium channels related to degenerins and epithelial sodium channels. *Proc. Natl. Acad. Sci. USA.* 94:1459–1464.

Gründer, S., H.S. Geissler, E.L. Bässler, and J.P. Ruppersberg. 2000. A new member of acid-sensing ion channels from pituitary gland. *Neuroreport.* 11:1607–1611.

Immke, D.C., and E.W. McCleskey. 2003. Protons open acid-sensing ion channels by catalyzing relief of Ca^{2+} blockade. *Neuron.* 37:75–84.

Kellenberger, S., I. Gautschi, and L. Schild. 1999a. A single point mutation in the pore region of the epithelial Na^+ channel changes ion selectivity by modifying molecular sieving. *Proc. Natl. Acad. Sci. USA.* 96:4170–4175.

Kellenberger, S., N. Hoffmann-Pochon, I. Gautschi, E. Schneeberger, and L. Schild. 1999b. On the molecular basis of ion permeation in the epithelial Na^+ channel. *J. Gen. Physiol.* 114:13–30.

Kellenberger, S., and L. Schild. 2002. Epithelial sodium channel/degenerin family of ion channels: a variety of functions for a shared structure. *Physiol. Rev.* 82:735–767.

McNicholas, C.M., and C.M. Canessa. 1997. Diversity of channels generated by different combinations of epithelial sodium channel subunits. *J. Gen. Physiol.* 109:681–692.

Palmer, L.G. 1985. Interactions of amiloride and other blocking cations with the apical Na channel in the toad urinary bladder. *J. Membr. Biol.* 87:191–199.

Price, M.P., P.M. Snyder, and M.J. Welsh. 1996. Cloning and expres-

sion of a novel human brain Na^+ channel. *J. Biol. Chem.* 271: 7879–7882.

Renard, S., E. Lingueglia, N. Voilley, M. Lazdunski, and P. Barbry. 1994. Biochemical analysis of the membrane topology of the amiloride-sensitive Na^+ channel. *J. Biol. Chem.* 269:12981–12986.

Schild, L., E. Schneeberger, I. Gautschi, and D. Firsov. 1997. Identification of amino acid residues in the alpha, beta, and gamma subunits of the epithelial sodium channel (ENaC) involved in amiloride block and ion permeation. *J. Gen. Physiol.* 109:15–26.

Sheng, S., J. Li, K.A. McNulty, D. Avery, and T.R. Kleyman. 2000. Characterization of the selectivity filter of the epithelial sodium channel. *J. Biol. Chem.* 275:8572–8581.

Sheng, S., K.A. McNulty, J.M. Harvey, and T.R. Kleyman. 2001. Second transmembrane domains of ENaC subunits contribute to ion permeation and selectivity. *J. Biol. Chem.* 276:44091–44098.

Snyder, P.M., F.J. McDonald, J.B. Stokes, and M.J. Welsh. 1994. Membrane topology of the amiloride-sensitive epithelial sodium channel. *J. Biol. Chem.* 269:24379–24383.

Snyder, P.M., D.R. Olson, and D.B. Bucher. 1999. A pore segment in DEG/ENaC Na^+ channels. *J. Biol. Chem.* 274:28484–28490.

Sutherland, S.P., C.J. Benson, J.P. Adelman, and E.W. McCleskey. 2001. Acid-sensing ion channel 3 matches the acid-gated current in cardiac ischemia-sensing neurons. *Proc. Natl. Acad. Sci. USA.* 98:711–716.

Ugawa, S., T. Yamamoto, T. Ueda, Y. Ishida, A. Inagaki, M. Nishigaki, S. Shimada, Y. Minami, W. Guo, Y. Saishin, et al. 2003. Amiloride-insensitive currents of the acid-sensing ion channel-2a (ASIC2a)/ASIC2b heteromeric sour-taste receptor channel. *J. Neurosci.* 23:3616–3622.

Waldmann, R., G. Champigny, N. Voilley, I. Lauritzen, and M. Lazdunski. 1996. The mammalian degenerin MDEG, an amiloride-sensitive cation channel activated by mutations causing neurodegeneration in *Caenorhabditis elegans*. *J. Biol. Chem.* 271:10433–10436.

Waldmann, R., G. Champigny, F. Bassilana, C. Heurteaux, and M. Lazdunski. 1997a. A proton-gated cation channel involved in acid-sensing. *Nature.* 386:173–177.

Waldmann, R., F. Bassilana, J. de Weille, G. Champigny, C. Heurteaux, and M. Lazdunski. 1997b. Molecular cloning of a non-inactivating proton-gated Na^+ channel specific for sensory neurons. *J. Biol. Chem.* 272:20975–20978.

Waldmann, R., and M. Lazdunski. 1998. H^+-gated cation channels: neuronal acid sensors in the NaC/DEG family of ion channels. *Curr. Opin. Neurobiol.* 8:418–424.

Woodhull, A.M. 1973. Ionic blockage of sodium channels in nerve. *J. Gen. Physiol.* 61:687–708.

Zhang, P., and C.M. Canessa. 2002. Single channel properties of rat acid-sensitive ion channel-1α, -2a, and -3 expressed in *Xenopus oocytes*. *J. Gen. Physiol.* 120:553–566.